ELSEVIER

Contents lists available at ScienceDirect

### BBA - Gene Regulatory Mechanisms

journal homepage: www.elsevier.com/locate/bbagrm





# Transposon insertion causes *ctnnb2* transcript instability that results in the maternal effect zebrafish *ichabod* (*ich*) mutation

Zsombor Varga <sup>a</sup>, Ferenc Kagan <sup>a,b</sup>, Shingo Maegawa <sup>c</sup>, Ágnes Nagy <sup>d</sup>, Javan Okendo <sup>e</sup>, Shawn M. Burgess <sup>e</sup>, Eric S. Weinberg <sup>f</sup>, Máté Varga <sup>a,\*</sup>

- a Department of Genetics, ELTE Eötvös Loránd University, Budapest, Hungary
- b Max Planck Institute for Multidisciplinary Sciences, Göttingen, Germany
- <sup>c</sup> Department of Intelligence Science and Technology, Graduate School of Informatics, Kyoto University, Japan
- <sup>d</sup> Hungarian Defence Forces Medical Centre, Budapest, Hungary
- e Translational and Functional Genomics Branch, National Human Genome Research Institute, Bethesda, MD, USA
- f Department of Biology, University of Pennsylvania, Philadelphia, PA, USA

#### ABSTRACT

The maternal-effect mutation *ichabod* (*ich*) results in ventralized zebrafish embryos due to impaired induction of the dorsal canonical Wnt-signaling pathway. While previous studies linked the phenotype to reduced *ctnnb2* transcript levels, the causative mutation remained unidentified. Using long-read sequencing, we discovered that the *ich* phenotype stems from the insertion of a non-autonomous CMC-Enhancer/Suppressor-mutator (CMC-EnSpm) transposon in the 3'UTR of the gene. Through reporter assays, we demonstrate that while wild type *ctnnb2* mRNAs exhibit remarkably high stability throughout the early stages of development, the insertion of the transposon dramatically reduces transcript stability. Genome-wide mapping of the CMC-EnSpm transposons across multiple zebrafish strains also indicated ongoing transposition activity in the zebrafish genome. Our findings not only resolve the molecular basis of the *ich* mutation but also highlight the continuing mutagenic potential of endogenous transposons and reveal unexpected aspects of maternal transcript regulation during early zebrafish development.

#### 1. Introduction

In sexually reproducing species, new life is initiated by the fusion of parental gametes, albeit the zygote is anything but a blank slate after fertilization. Oocytes are loaded with maternal factors, mRNAs and proteins, which drive the developmental processes during the earliest stages of embryogenesis, until transcription from the embryo's own genome is turned on. The length of this stage and the timing of the so called maternal-zygotic-transition (MZT), which effectively terminates this early stage of development, is highly species-dependent [1,2]. In those species where several cell cycles elapse before MZT, usually the oocytes are already highly patterned themselves. Consequently, the maternal factors will not only coordinate early cell divisions but will also have a significant role in the initial patterning of the embryonic axes [3,4].

The importance of maternal genes was established during the initial dissection of the early metazoan development using forward genetics in fruit flies (*Drosophila melanogaster*) (reviewed in [5,6]. Subsequent genetic screens in zebrafish (*Danio rerio*), recently complemented by "crispant" screens, have also identified numerous important maternal

effect genes [7-10]. Some maternal mutants, such as ich [11] or tokkaebi (tkk) [12,13] were also uncovered independently of forward mutagenesis.

The mapping and characterization of these maternal mutants (in parallel with other experiments) revealed the intricate relationship between the maternal factors asymmetrically segregated along the animal-vegetal axis and the dorsal-specific activation of the canonical Wnt/ $\beta$ -catenin signaling pathway, which occurs in early blastula stages [4,14]. Fertilization of the zebrafish egg is followed by a cortical rotation, which will move the vegetally located dorsal determinant (likely *wnt8a* mRNA) to the future dorsal side of the developing embryo [15–17]. This relocation is essential for the timely activation of the canonical Wnt pathway and the nuclear localization of  $\beta$ -catenin [15,18].

The maternal-effect *ich* mutation results in ventralized embryos, due to impaired induction of dorsal canonical Wnt-signaling, resulting from reduced transcription levels of *ctnnb2*, encoding zebrafish  $\beta$ -catenin-2 (Ctnnb2) [19]. This property makes it particularly well suited to study early dorsal patterning events in development [20–26]. Of note, the mutation can be completely rescued by the injection of *ctnnb2* mRNA, *ctnnb1* mRNA or *Xenopus*  $\beta$ -catenin mRNA as well [11].

E-mail address: mvarga@ttk.elte.hu (M. Varga).

<sup>\*</sup> Corresponding author.

While genetic mapping of the *ich* allele suggested that the mutation resides in the proximity to *ctmb2*, no mutation was found in the coding sequence (CDS) of the gene in *ich* homozygotes. Furthermore, the telomeric location of the *ctmb2* locus frustrated previous attempts to positionally clone the mutation [19].

Ever since their discovery in the middle of the 20th century [27], transposable elements (TEs) have been recognized as potent biological mutagens capable of disrupting the normal function of genes in a variety of organisms [28]. Indeed, some historically relevant phenotypes, such as the wrinkled peas of Mendel [29] or the melanized forms of the peppered moths which appeared during the Industrial Revolution in 19th century Britain [30] were the result of transposon insertions. The mobility of these "jumping genes" have also made them a prime tool for transgenic technologies in multiple model species, including zebrafish [31–35].

Vertebrate genomes carry varying levels of TEs, and in some species such as zebrafish and humans over half of the genome can consist of such sequences [36,37]. DNA transposons as type II TEs are in general enriched within the zebrafish genome and CMC EnSpm transposons constitute one of the largest family amongst them [36–39].

Using a long-read genomic sequencing approach, here we show that the *ich* phenotype results from the insertion of an EnSpm-type transposon into the 3'UTR of the *ctnnb2* gene, which causes the degradation of an otherwise very stable maternal transcript.

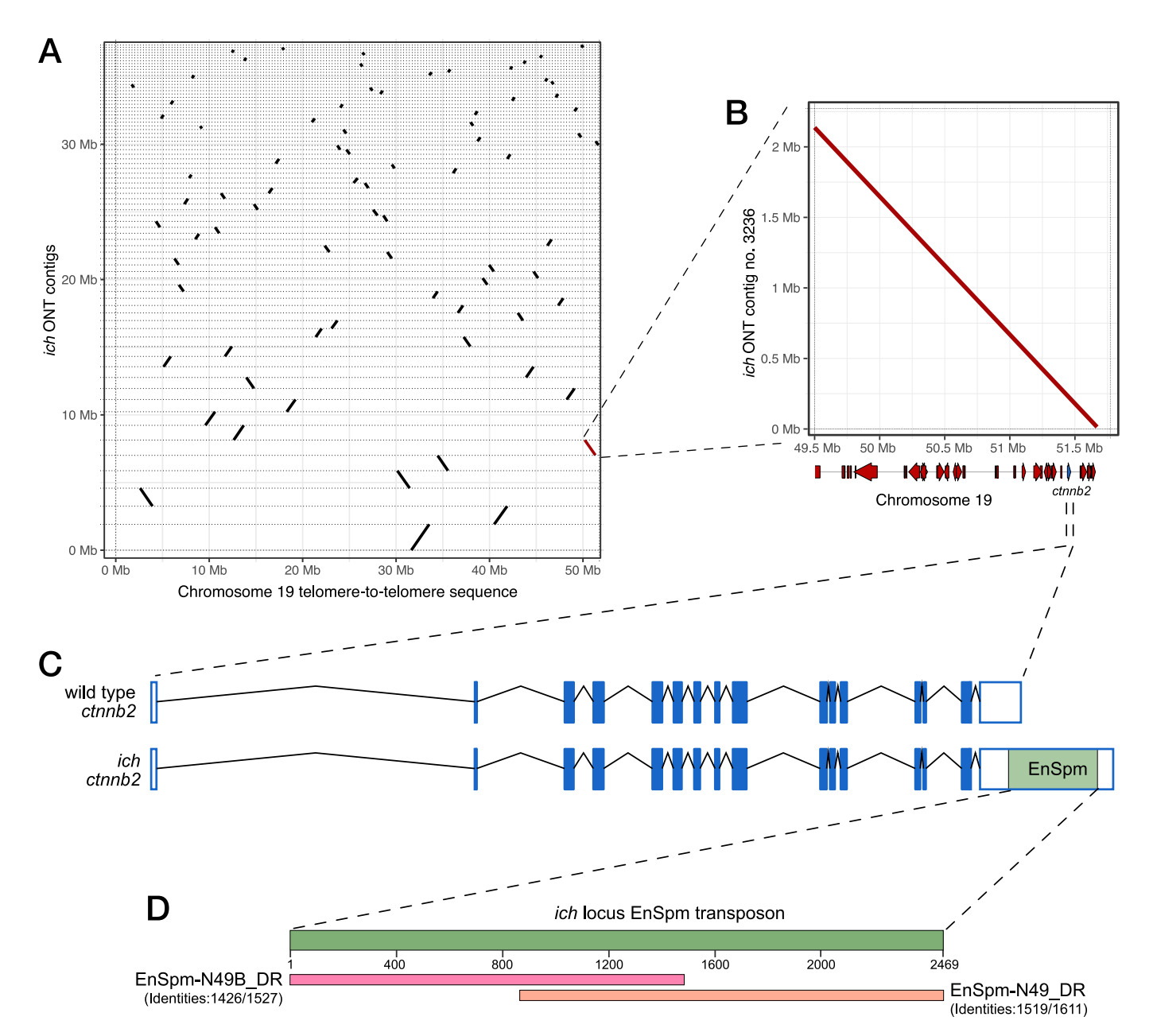


**Fig. 1.** Long-read sequencing identifies an EnSpm transposon in the 3'UTR of *ctmb2* in *ich* animals. (A) Dotplot representation of different *ich* contigs that could be aligned to the "telomere-to-telomere" sequence of the zebrafish chromosome 19. The highlighted (red) contig contains the genomic region of the *ctmb2* gene. (B) Dotplot comparison of the relevant *ich* contig and the telomeric portion of chromosome 19 reveals no genomic rearrangement in this region in *ich* animals. Gene position schematics are visible along the horizontal axis. (C) Comparison of wild-type and *ich*-specific *ctmb2* sequences showing the position of the EnSpm-type transposon insertion. (D) BLAST results of the *ich*-specific transposon in the FishTEDB [40].

#### 2. Results

### 2.1. A transposon insertion can be observed in the 3'UTR of ctnnb2 in ich mutants

Earlier positional cloning experiments placed the causative mutation of *ich* in close proximity to the *ctnnb2* locus, and while no mutations could be uncovered in the CDS of the gene, maternal levels of *ctnnb2* mRNA and Ctnnb2 protein were severely reduced in the embryos of homozygous females [19].

To determine the exact physical nature of the causative mutation, we conducted Oxford Nanopore Technologies (ONT) long-read sequencing on one homozygous *ich* female. We have assembled the ONT reads into contigs and aligned the resulting contigs to a newly assembled, "telomere-to-telomere" sequence of chromosome 19 (GCA\_033170195.2) and selected the contig that spanned the *ctnnb2* locus (Fig. 1A,B). The alignment of this 2.27 Mbp long contig to the reference genome sequence showed no sign of structural variation, thus proceeded to a manual annotation of the *ctnnb2* locus. This annotation revealed the presence of a 2469 bp long insertion in the last exon of the gene, within

the 3'UTR region (Fig. 1C).

A closer examination of this insertion revealed that it is a hybrid sequence between two previously recognized, non-autonomous CMC-EnSpm type transposons: EnSpm-N49\_DR and EnSpm-N49B\_DR (Fig. 1D) [40]. This hybrid transposon has a 15 bp long terminal inverted repeat (TIR) identical to the one described for EnSpm-N49B\_DR (CACTCAAAAAAATGA) and creates a CA target site duplication.

With allele-specific primers, we were able to confirm that in all *ich* homozygous females both *ctnnb2* alleles carried this insertion (Supplementary Fig. 1).

#### 2.2. ctnnb2 transcripts show high stability during early development

Previous work has already highlighted that while the *ich* mutation causes a reduction in the level of *ctnnb2* transcripts, the phenotype itself can be rescued not only by the injection of *ctnnb2* mRNA, but also *ctnnb1* mRNA can rescue the phenotype [19]. Zebrafish Ctnnb1 and Ctnnb2 are highly similar proteins, with slight differences detected only in the Cterminal region (Supplementary Fig. 2A,B). The transcripts of the two orthologs also show high similarity within their coding regions and

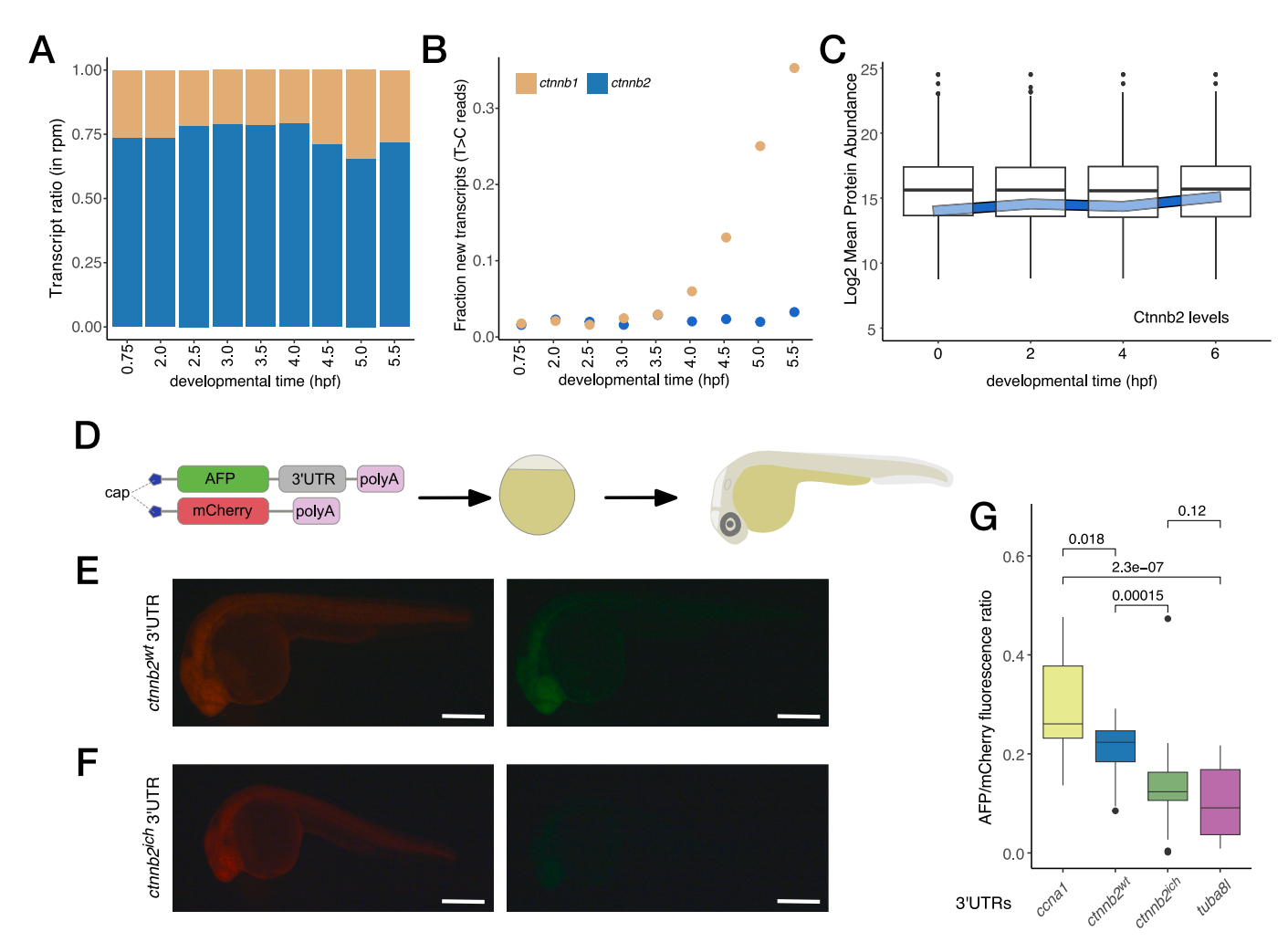


Fig. 2. High stability of maternal *ctnnb2* transcripts is disrupted by 3'UTR transposon insertion. (A) Transcriptome analysis of maternal *ctnnb1* and *ctnnb2* mRNAs shows a heightened abundance of maternal *ctnnb2* transcripts throughout early development (rpm – reads per million bp, *ctmb1* transcripts are shown in beige, *ctnnb2* transcripts in blue). (B) Metabolic labelling suggests active transcription of *ctnnb1* after ZGA, but no expression of *ctnnb2*. (Data for panels A and B are derived from [41]. (C) Maternal Ctnnb2 protein levels are also very stable during early stages of development as compared to mean protein abundances at these timepoints. (Data from [43]. (D) Experimental scheme used to test the effect of 3'UTRs on the stability of mRNAs. *In vitro* transcribed *AFP* mRNAs with different 3'UTRs are combined with *mCherry* transcripts with invariant 3'UTRs and injected into 1-cell stage zebrafish embryos. Fluorescence intensity for both AFP and mCherry is measured at 24 hpf. (E, F) Typical fluorescence observed in embryos injected with *AFP* carrying *ctnnb2*<sup>wt</sup> or *ctnnb2*<sup>ich</sup> 3'UTRs, respectively. (Scale bars: 0.5 mm) (G) Relative fluorescence intensities observed in embryos injected with different 3'UTRs compared to stable and unstable controls (*ccna1* and *tuba8l* 3'UTRs, respectively). (Pairwise *p* values were calculated with the Kruskal-Wallis test.)

5'UTRs (83.11 % identity). Sequence comparisons, however, show that the 3'UTR of the two genes is highly divergent, with no similarities to be found (Supplementary Fig. 2C). As both paralogs are also transcribed during oogenesis (Supplementary Fig. 3D), the difference in the 3'UTRs suggested that one plausible explanation for the inability of endogenous *ctnnb1* to rescue *ich* would be a difference in the stability of *ctnnb1* and *ctnnb2* maternal transcripts.

Until recently, the lack of adequate labelling and detection methods prevented scientists from understanding how maternal and zygotic gene products change during the MZT in developing embryos. Newly available datasets that rely on metabolic labeling to differentiate between maternal and zygotic transcripts and assess maternal protein stability [41–43], however, gave us new opportunities to compare the expression of *ctnnb1* and *ctnnb2* at high resolution during the early development of wild-type embryos.

Interestingly, we observed that ctnnb2 transcripts are about three times as abundant as ctnnb1 ones both pre- and post-MZT in wild-type embryos (Fig. 2A), even though no zygotic transcription can be detected from ctnnb2 (Fig. 2B). Similarly, Ctnnb2 levels also seem constant during these early stages of development (Fig. 2C), which also include the 256-cell stage (2.5 hpf), the earliest timepoint when nuclear  $\beta$ -catenin can be detected in the dorsal side of the zebrafish blastula [44,45]. Of note, while protein profiling datasets did not report Ctnnb1 stability [43], earlier observations using a pan- $\beta$ -catenin antibody showed that maternal Ctnnb1 is present in both wild-type and ich embryos [19,46].

## 2.3. Transposon insertion in the 3'UTR disrupts the stability of ctnnb2 transcripts

To test if the insertion of the hybrid EnSpm transposon in the 3'UTR destabilizes the *ctnnb2* we utilized a previously described reporter assay [47]. We co-injected *in vitro* synthesized *AFP* mRNAs with varying 3'UTRs and *mCherry* with non-variant 3'UTRs in wild type embryos and estimated the ratio of AFP and mCherry intensity in these embryos at 24 h post fertilization (hpf) (Fig. 2D).

We measured intensities for constructs carrying either the wild-type or the *ich*-specific *ctnnb2* 3'UTRs and compared them to the well-established stable and unstable 3'UTRs of *ccna1* and *tuba8l*, respectively [47]. These results show that while the stability of wild type *ctnnb2* 3'UTR is comparable to that of the extremely stable *ccna1* 3'UTR, the insertion of the EnSpm transposon resulted in a dramatic reduction in the stability of the transcript, making it similar to that observed for *tuba8l*.

The 3'UTR of the wild-type *ctnnb2* gene is relatively long and carries a number of secondary structural motifs (Supplementary Fig. 3A), that could either stabilize the transcript by themselves, or could serve as platforms for interaction with RNA-binding proteins (RBPs) that regulate the stability of the mRNA [48]. To reveal if the insertion of the transposon could introduce any destabilizing sequence motifs in the 3'UTR, we took advantage of a random forest model to compare the predicted stabilities of the different *ctnnb2* 3'UTR sequences with the *ctnnb1* 3'UTR [49]. Interestingly, this analysis did not reveal any destabilizing motifs within the transposon itself, therefore the observed decrease in transcript stability is most likely not due to the potential destabilizing effects of particular sequences within the transposon itself (Supplementary Fig. 3B).

Active transposons are often the target of piRNA-driven destruction during zebrafish germ-cell development and embryogenesis [50–53], which offers another possibility for the premature degradation of maternal *ctnnb2* mRNAs. To test if this could be a feasible explanation for *ich* embryos, first we looked at the temporal dynamics of EnSpm-N49/N49B transcription. The reanalysis of previously published transposon expression datasets [54] shows that these particular transposons become active around the time of the zygotic genome activation (ZGA) but become downregulated shortly after. The decrease in the levels of EnSpm-N49/N49B transcripts around shield stage is concomitant with

an increase in the amount of piRNAs [53], suggesting a Piwi-dependent silencing mechanism, which, therefore, could provide a possible explanation for the degradation of the *ich*-specific *ctmb2* transcript as well.

#### 2.4. Active EnSpm-type elements in the zebrafish genome

Our mapping results revealed the recent disruption of the *ctnnb2* 3'UTR in *ich* animals due to the transposition of a hybrid EnSpm-N49/N49B-type transposon. As this suggested that the transposon is still active, we decided to map the location of EnSpm-N49, EnSpm-N49B and EnSpm-N49/49B transposons in the zebrafish reference genome and compare it to other, recently sequenced wild-type strains.

Our results suggest that of the three transposons the hybrid one appears to be the most active, as we were able to detect 72 copies in the GRCz11 reference genome, whereas only 7 copies of EnSpm-N49 and 16 copies of EnSpm-N49B were detected using an 80 % sequence similarity threshold (Fig. 3A, Supplementary Fig. 4A). Our analysis also shows higher sequence similarity for EnSpm-N49/N49B copies than for the other transposons, suggesting that this particular transposon is evolutionarily novel (Supplementary Fig. 4A). The genomic distribution of all three transposons is relatively similar, with most copies found in distal intergenic or intronic regions (Supplementary Fig. 4B—D).

To compare the positions of the investigated transposons between different wild-type strains, we also determined the location of the transposons in AB, Cooch Behar (CB), Nadia (NA) and T5D strains [55,56]. Our results confirm that the hybrid EnSpm-N49/N49B appears to be the most active of the three transposons (Supplementary Fig. 4E-H), and also reveal that all three transposons are actively transposing in the zebrafish genome as they show divergent distributions in the different isolates (Fig. 3B,C).

#### 3. Discussion

The mobility and hence the mutagenic potential of mobile genetic elements has been obvious since their discovery in maize [27] and it is now recognized as a general feature all organisms [28]. The molecular characterization and in-depth understanding of the transposition process has also made it possible to use such "selfish genetic elements" in biotechnology and numerous transgenesis methodologies have been developed that exploit the mobility of these sequences essentially in all model organisms [31–34]. Thanks to the related expansion of the genetic toolbox over the years numerous zebrafish mutant lines have been identified resulting from retroviral- or transposon-based mutagenesis screens [57–59].

Besides exogenous mobile elements, however, endogenous ones can also have mutagenic effects. Indeed, over the past decades several zebrafish mutant alleles known to be caused by spontaneous insertion of endogenous transposons have been also identified [13,60]. The sudden expansion of type II DNA transposons, in general, and CMC EnSpm transposons, in particular, in the zebrafish genome has expanded the repertoire of putative biological mutagens in this species [36–39]. While the mechanistic details of these transposon invasions have not been revealed, previous studies from other organisms suggest that type II transposons can multiply by moving during DNA replication and/or exploiting host repair mechanisms that inadvertently restore them at excision sites while they integrate elsewhere [61].

As shown by our results characterizing the *ich* allele, at least some of the CMC Spm transposons are still active (Fig. 3, Supplementary Fig. 4) and exert a mutagenic influence. The EnSpm-N49/N49B is a non-autonomous transposon, which requires the transposase activity of an autonomous element for its mobilization. A recent analysis of the zebrafish pangenome has highlighted a large, autonomous CMC EnSpm element with an intact transposase and multiple copies in the genome, which has an almost identical terminal inverted repeat (CACT-CAAAAAAAT) to the one observed in our case [62].

While TEs are often enriched on chromosome 4, the ancestral sex-

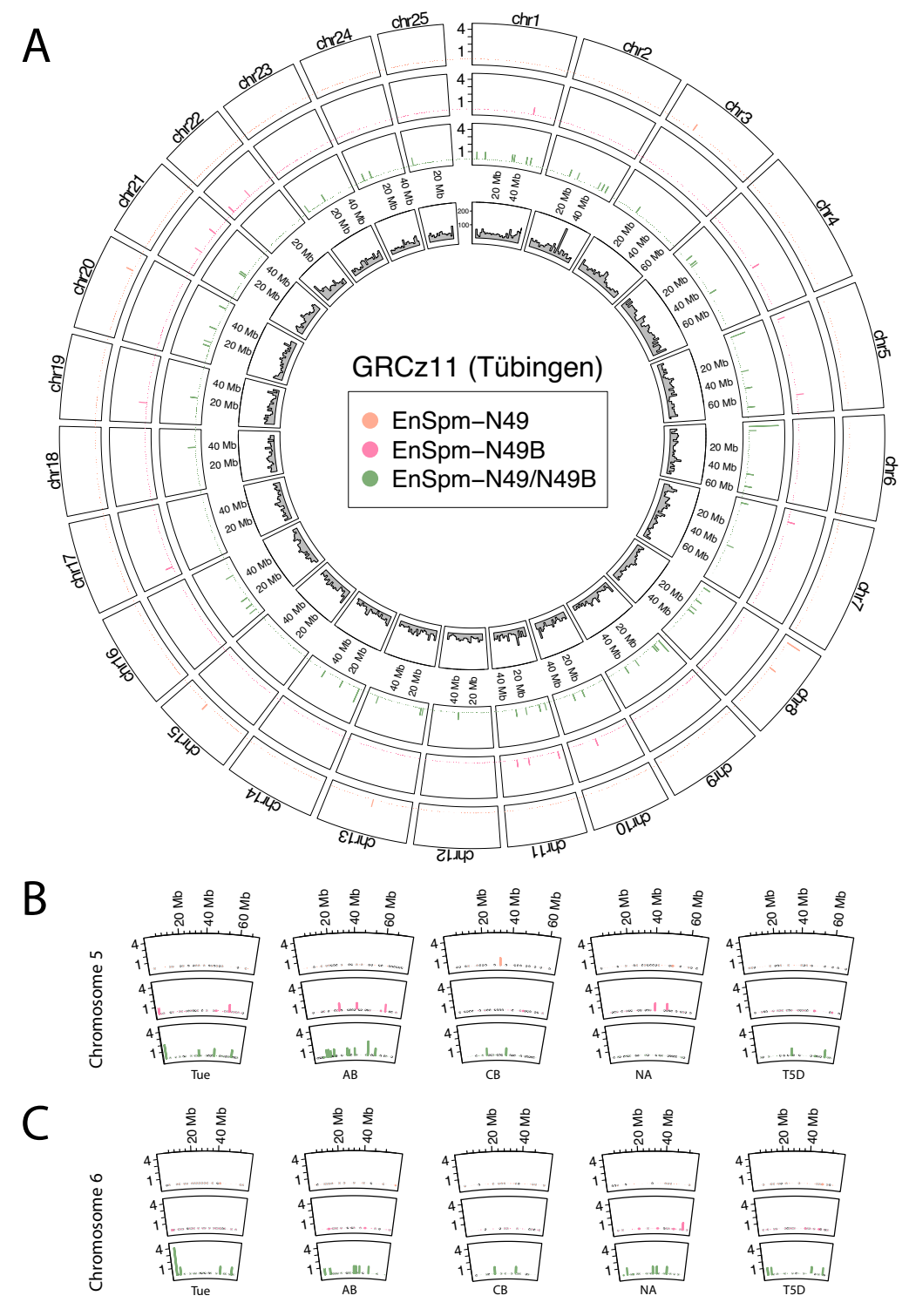


Fig. 3. The position of EnSpm transposons observed in this study vary across zebrafish genomes. (A) Genomic positions of EnSpm-N49 (orange), EnSpm-N49B (pink) and EnSpm-N49/N49B (green) transposons in nonoverlapping 2-Mbp windows across the nuclear chromosomes of the Tübingen (Tue) GRCz11 reference genome. Inner circle shows the coverage of protein-coding genes on the same chromosomes. (B, C) Genomic positions of the observed transposons show variability across the genomes of multiple wild-type isolates for chromosomes 5 (B) and 6 (C). (Y axis denotes copy numbers in the 2-Mbp windows. Strain abbreviations can be found in Table 3. For other chromosomes see Supplementary Fig. 4.)

chromosome of zebrafish with an abundance of transposable elements [54,63,64], and the accumulation of CMC EnSpm transposons has been also associated with the evolution of sex chromosomes in some other species [65], we do not see an enrichment of the three observed transposons on chromosome 4.

Admittedly, the fluorescent reporter assay we use to demonstrate the

destabilization of *ctnnb2* transcripts due to the insertion of a EnSpm-N49/N49B transposon sequence in exon 16 of the gene, containing the 3'UTR (Figs. 1 and 2), is a synthetic one, but it has been shown previously to report accurately the effect of 3'UTR sequences of transcript stability [47].

The observed destabilizing effect of the transposon also highlights

that despite years of rapid advances, our understanding of the processes that regulate the stability and turnover of mRNAs is still incomplete. Previous work has already highlighted that the presence of miR-430 binding sites [47,66], the codon composition of the CDS [67,68], the presence of specific structural elements in the transcript 3'UTRs [49,69] as well as the length of the polyA tail [70] can all have essential roles in regulating mRNA stability during MZT. As the transposon insertion does not appear to introduce destabilizing structures into the 3'UTR (Supplementary Fig. 3), in the case of the *ctnnb2*<sup>ich</sup> allele some other mechanistic explanation is needed, and the piRNA-dependent degradation of the TE-containing mRNA offers a plausible mechanism.

The Piwi-piRNA pathway provides a small RNA-based adaptive defence against TEs in most eukaryotic genomes [71–73]. It has especially important roles in containing these biological mutagens during the development of the gametes in most animals and zebrafish is no exception [50–52]. Elevated activity of the Piwi-piRNA pathway during oogenesis and could provide a possible mechanistic explanation for the degradation of the  $ctnnb2^{ich}$  transcripts, which contain a perfect transposon target.

It is also worth highlighting the high stability of the wild-type maternal *ctnnb2* transcript. Even in the absence of a zygotic component, there seem to be approximately three times as many *ctnnb2* transcripts as those of *ctnnb1* during early development (Fig. 2). This does not appear to be caused by differential stability of 3'UTRs as based on this sequence alone, and *ctnnb1* transcripts should be at least as stable as their *ctnnb2* counterparts (Supplementary Fig. 3).

This makes it likely that an interaction with yet unknown RNA-binding proteins (RBPs) is behind the observed stability levels. It is noteworthy, however, that a screen of putative RNA binding sites [74] did not highlight any obvious candidates that would account for the differential stability of *ctnnb1* and *ctnnb2* (not shown). Understanding the causes for the high stability of *ctnnb2* transcripts, therefore, could provide important additional information about the mechanisms that preserve transcripts during oogenesis and protect them from degradation during ZGA, when typically, we see the turnover of maternal transcripts to zygotic ones.

In summary we have identified the insertion of an EnSpm transposon in the 3'UTR of the *ctnnb2* gene as the most likely proximate cause of *ctnnb2* transcript instability observed in the embryos of homozygous *ich* mutant fish. We showed that the transposon-containing *ctnnb2* 3'UTR is considerably less stable than the wild-type counterpart. We also describe the genomic distribution of the transposon in multiple zebrafish genomes, providing evidence about the recent activity of this TE.

#### 4. Materials and methods

#### 4.1. Fish husbandry and maintenance

Adult wild-type (*ekwill*) and *ich* (*ctmb2*<sup>p1</sup>) fish used for these experiments were maintained and bred in the animal facility of the Biology Institute of ELTE Eötvös Loránd University according to existing protocols [75,76]. Experiments were carried out in accordance with the Hungarian Act of Animal Care and Experimentation (1998, XXVIII) and with the directive 2010/63/EU of the European Parliament and of the Council of 22 September 2010 on the protection of animals used for scientific purposes. All animal husbandry protocols used for this study were approved by the ELTE Animal Welfare Animal Committee and the Hungarian National Food Chain Safety Office (PEI/001/1713–2/2015) and by the Animal Experiment Committee of Kyoto University (Inf—K25001).

#### 4.2. Genomic DNA isolation and long-read sequencing

Total genomic DNA was isolated from a homozygous *ich* female specimen (weighing approximately 50 mg) stored in DNA/RNA Shield Reagent (Zymo Research, cat # R1100) using a DNeasy Blood and Tissue

Kit (Qiagen, cat # 69504) in accordance with the manufacturer's protocol for Purification of Total DNA from Animal Tissues, with some modifications. The fish was split in two halves, the first sample containing the anterior part, the second the posterior part (mostly body muscle and skin). A total of 360  $\mu$ l of ATL buffer and 40  $\mu$ l of proteinase K were added to the samples, which were then vortexed rigorously. The mixtures were then incubated at 56 °C for 3.5 h with 400 rpm mixing and vortexing every 30 min. Thereafter, 400 µl of AL buffer and 400 µl of ethanol were added to the lysates, which were then vortexed vigorously and subsequent steps were then continued according to the manufacturer's protocol. Two sequencing libraries were prepared with the Ligation Sequencing Kit SQK-LSK110 (Oxford Nanopore Technologies, Oxford, cat # SQK-LSK110) according to the manufacturer's protocol for genomic DNA by ligation, with  $1.5 \mu g$  of input from both genomic DNAs being added to each library preparation. The entire quantity of each prepared library (1st library: 680 ng, 2nd library: 39.6 ng) was loaded in 75 µl volume onto two R9.4.1 flow cells (Oxford Nanopore Technologies, cat # FLO-MIN106) and run for 48 h until flow cell extinction. Sequencing data were generated using the Oxford Nanopore GridION platform and performing real-time super-accurate basecalling with MinKNOW 23.04.5 and Guppy 6.5.7 (Oxford Nanopore Technologies, Oxford, UK) to achieve the highest possible accuracy rate. The sequencing runs generated a total of 28.19 Gb of raw genomic data in two batches.

#### 4.3. Genome assembly and analysis

Raw ONT data was uploaded into the <a href="https://usegalaxy.eu">https://usegalaxy.eu</a> platform [77]. For assembly of contigs we used the Fly assembler [78], and later performed scaffolding based on the GRCz11 reference genome sequence using RagTag [79]. This scaffolding step allowed us to select for those ich contigs that contained genomic sequences specific for chromosome 19. These sequences were aligned along the chromosome-to-chromosome sequence of chromosome 19 using minimap2 [80]. The settings used to run these programs are presented in Table 1. The contig containing the genomic neighborhood (contig no. 3236) was annotated manually in the Benchling online software suite [81].

#### 4.4. Genomic DNA isolation for genotyping PCRs

PCR-ready genomic DNA isolation was performed as described before [82]. Briefly, after anesthesia, each fish was fin-clipped and tissue samples were transferred to a 200  $\mu l$  PCR tube. After the addition of 100  $\mu l$  of 50 mM NaOH solution the samples were heated at 95 °C for 15 min with occasional flicking. Subsequently, the tubes were cooled down to 4 °C and lastly 10  $\mu l$  of 1 M Tris-HCl (pH 8.0) was added for balancing the pH to near-neutral.

#### 4.5. Genotyping PCR of ich fish

Exon 16-specific genotyping PCRs were performed on six adult fish and ten embryos, using with the following three primer pairs (Fig. S1A): (1) the ctnnb2\_ex16 primer pair, ctnnb2\_ex16\_L (5'-TCCGTGTTTCCCA-GAAGAAGC-3') and ctnnb2\_ex16\_R (5'-GAAAGTGCCTGATGAGTGCG-3'), (2) the ctnnb2\_ex16\_tp primer pair, ctnnb2\_ex16\_tp\_L (5'-GAAAGTGCCTGATGAGTGCC-3')

 Table 1

 Standard parameters used in the usegalaxy.eu pipeline.

Software package	Parameters used
Fly RagTag	-nano-raw./input_0.fastq.gz -o out_dir -t -i 1 scaffold -u -aligner minimap2 -mm2-params '-k19 -w19 -A1 -B19 -O39,81 -E3,1 -s200 -z200 -min-occ-floor = 100' -f 1000 -remove-small -q 10 -d 100,000 -i 0.2 -a 0.0 -s 0.0 -r -g '100' -m '100000' -o./ -t
minimap2	-x asm5 -q-occ-frac 0.01 -t

CTAGGATCCGTTTGTCAAGCCCACACACC-3') and ctnnb2 ex16 tp R (5'-GATGAATTCCTCATGGTACTGACCCGAGC-3'), (3)ctnnb2 ex16 whole primer pair, ctnnb2 ex16 whole L (5'-GCGTGTGGTTAATCGTCTGC-3') and ctnnb2\_ex16\_whole\_R GAGTTCTGTCTGATCGGGCC-3'). PCR reaction was performed with Primestar HS DNA polymerase (Takara, cat # R10A) with the following settings: one cycle of initial denaturation at 98 °C for 1 min, 30 cycles of denaturation at 98 °C for 10 s, and extension at 68 °C for 3 mins. Genotyping PCRs spanning intron 15 were performed on five additional ich homozygous adults and one adult wild type (AB) fish. In these reactions the following primer pairs were used: ctnnb2\_ex15\_F (5'-TCCAAT-CAGCTGGCCTGGTTCG-3') in combination with either ctnnb2 ex16 R (5'-CGTCTGCCAGCTCTACTTCCCC-3') for the amplification of the wild type allele, or ich\_DR\_R (5'-GGTAACTTAACTCGGTTACGTGG-3') for the amplification of the ich allele. PCR reactions were done using Thermo Scientific DreamTaq DNA Polymerase (cat # EP0711), using the following settings: 1 cycle of initial denaturation on 95 °C for 3 min, 32 cycles of denaturation on 95 °C for 30 s, annealing on 66 °C for 30 s and extension on 72  $^{\circ}$ C for 37 s, and 1 cycle of final extension on 72  $^{\circ}$ C for 7 min.

#### 4.6. Synthesis and cloning of 3'UTRs

For RT-PCR, total RNA was isolated from 1 to 8 cell wild-type and ich zebrafish embryos, using Zymo TRI Reagent (ZYMO Research, cat # R2050-1-50) as briefly follows: 20 embryos were collected in a 1.5 ml tube, and excess medium was removed. The samples were homogenized in 0.5 mL TRI Reagent, incubated for 5 min, mixed with 100  $\mu l$  chloroform, and centrifuged at  $10,000 \times g$  for 15 min at 4 °C. The aqueous phase was transferred to a new tube, mixed with 250  $\mu l$  isopropanol, and incubated for 10 min. After centrifugation, the RNA pellet was washed with 70 % ethanol, air-dried for 5–10 min, and dissolved in nuclease-free water.

Isolated total RNA was applied as template for cDNA synthesis, using the SuperScript IV UniPrime One-Step RT-PCR System (Invitrogen, cat # 12597025) according to manufacturer's protocol. Wild-type RNA template was used for *ccna1*, *ctnnb2* and *tuba8l*, *ich* RNA for *ich-ctnnb2* with primers in Table 1.

Wild-type 3'UTRs were then cloned into pCS2 + MT-AFP expression vector, where a S65A/Y145F mutated, humanized form of GFP, with improved fluorescent intensity is expressed from an SP6 promoter [83]. In the case of *ccna1* and *tuba81* 3'UTRs, the DNA fragments were stickyend ligated into *Xho*I and *Xba*I sites with T4 DNA Ligase (Thermo Scientific, cat # EL0014). Wild-type *ctnnb2* 3'UTR was blunt-end ligated into *Stu*I site in the same manner. All three ligations were then transformed into *E. coli* DH5a competent cells and selected on ampicillin containing LB plates. After inoculation and growth, miniprep was performed with GeneJET Plasmid Miniprep Kit (Thermo Scientific, cat # K0502). All plasmids were sent for sequencing for the verification of proper cloning.

Probably due to the low quality of total RNA template, we were not able to amplify the whole  $ctnnb2^{ich}$  3'UTR in one piece and hence we did the amplification in two steps as follows:

First, using ctnnb2\_ex16-XbaI-R1 and ich-ctnnb2-F1 (Table 2) primers, we amplified a 1410 bp long fragment and blunt-end cloned into a *Eco*RV-linearized pBluescript KS(+) plasmid. ich-ctnnb2-F1 was designed to be specific to a region on the *ich* locus where it can have an ATC nucleotide triplet on its 5' end. In this way, it is able to complete the residue of *Eco*RV recognition site on the pBluescript KS(+) plasmid, allowing us to perform another round of *Eco*RV digestion and blunt-end cloning of the second half of *ich-ctnnb2* 3'UTR (a 2114 bp long fragment amplified with ctnnb2\_ex15-XhoI-F1 and ich-ctnnb2-R2 primers). After the completion of cloning, *ctnnb2*<sup>ich</sup> 3'UTR containing pBluescript KS(+) was double-digested with *Xho*I and *Xba*I, which was followed by the gel isolation of *ctnnb2*<sup>ich</sup> 3'UTR and sticky-end ligation into pCS2+MT-AFP expression vector (as previously described).

**Table 2**Primers used for 3'UTR amplifications. For *ccna1* and *tuba8l* 3'UTR, the primers were implemented from [47].

Primer name	Sequence (5'-3')	
ccna1-3'UTR-F	AAACTCGAGTCCCAGTTGGAACCTGTAGA	
ccna1-3'UTR-R	AAATCTAGACTTGTTTCATTTATAAAAAGGCAGT	
ctnnb2_ex15-F1	TCCAATCAGCTGGCCTGGTTCG	
ctnnb2_ex16-R1	CGTCTGCCAGCTCTACTTCCCC	
ctnnb2_ex15-XhoI-F1	ATATCTCGAGTCCAATCAGCTGGCCTGGTTCG	
ich-ctnnb2-R2	CGTCCAGGTACTATGCCTTTAGATGCC	
ich-ctnnb2-F1	ATCCACAGTCTCCTCAGCCAGATATGG	
ctnnb2_ex16-XbaI-R1	ATATTCTAGACGTCTGCCAGCTCTACTTCCCC	
tuba8l-3'UTR-F	AAACTCGAGTGCTTCAAAAAGCTGATCTGAG	
tuba81-3'UTR-R	AAATCTAGACAATTTATTCTGAAACTGCATTGA	

#### 4.7. mRNA synthesis

3'UTR containing pCS2+MT-AFP and unmodified pCS2+mCherry expression vectors were linearized with *Not*I and transcribed with mMESSAGE mMACHINE™ SP6 Transcription Kit (Invitrogen, cat # AM1340) following the manufacturer's protocol. mRNA samples were purified with phenol:chloroform extraction and isopropanol precipitation method (according to the manufacturer's protocol).

#### 4.8. Embryo injections and quantification of fluorescent signal

Wild type (*ekwill*) embryos were injected with 1 nl of the mixture of *AFP-3'UTR* and *mCherry* mRNAs at one cell stage. The concentration of *AFP-3'UTR* and *mCherry* mRNAs were 140 ng/ $\mu$ l and 100 ng/ $\mu$ l, respectively. At ~24 hpf we documented AFP- and mCherry-expressing fish using a Zeiss Lumar.v12 UV stereomicroscope. In average 20 embryos were photographed for each injection. For the evaluation of relative fluorescent protein brightness, we utilized Fiji [84].

#### 4.9. Screening of multiple D. rerio genomes for TE insertion

Transposable element sequences were retrieved from FishTEDB [40]. Multiple *D. rerio* genomes (Table 3) were screened for the presence of EnSpm-N49\_DR, EnSpm-N49B\_DR, and the hybrid of the two, EnSpm-N49/N49B\_DR. The screening was performed using the BLAST search algorithm [85] with default settings.

Screening results were further processed using custom scripts. TE hits were filtered downstream of the analysis for e-value of  $1e^{-10}$ . To alleviate spurious hits, a further filtering step was introduced whereby only hits where 80 % of the transposable element was mappable were retained. All downstream analyses were performed on the hits retained after the filtering steps outlined above. Genome-wide insertion events were analyzed using *Granges* [86], and visualized using *circlize* [87]. Annotation of the insertion sites was performed using *ChIPSeekR* [88,89].

#### 4.10. Statistics and visualization

Statistical analysis and visualization were performed in R [90] using the *ggplot2* package [91]. All figures have been assembled in Affinity Designer (Serif Europe).

**Table 3**Genome assemblies screened for the presence of transposable elements.

NCBI RefSeq assembly	Strain	Abbreviation used
GCF_000002035.6 (reference)	Tübingen	Tue
GCA_018400075.1	T5D	T5D
GCA_020184715.1	AB	AB
GCA_903798175.1	Nadia	NA
GCA_903798165.1	Cooch Behar	CB
GCA_033170195.2	Tübingen	T2T

#### CRediT authorship contribution statement

Zsombor Varga: Writing - review & editing, Writing - original draft, Investigation. Ferenc Kagan: Writing - review & editing, Writing original draft, Methodology, Investigation, Data curation. Shingo Maegawa: Writing - review & editing, Writing - original draft, Investigation, Conceptualization. Agnes Nagy: Writing - review & editing, Writing - original draft, Methodology, Investigation. Javan Okendo: Methodology, Data curation. Shawn M. Burgess: Writing - review & editing, Writing - original draft, Funding acquisition, Data curation. Eric S. Weinberg: Writing – review & editing, Writing – original draft, Conceptualization. Máté Varga: Writing - review & editing, Writing original draft, Visualization, Supervision, Project administration, Methodology, Investigation, Funding acquisition, Data curation, Conceptualization.

#### Declaration of competing interest

The authors declare that they have no known competing financial interests or personal relationships that could have appeared to influence the work reported in this paper.

#### Acknowledgements

We would like to thank Anita Rácz for fish care. This work was supported by the ELTE Eötvös Loránd University Institutional Excellence Program Grant 1783-3/2018/FEKUTSRAT. MV is a János Bolyai fellow of the Hungarian Academy of Sciences (BO/00555/22/8). This research was supported in part by the Intramural Research Program of the National Human Genome Research Institute (ZIAHG000183-24). The authors also acknowledge the support of the Freiburg Galaxy Team: Björn Grüning, Bioinformatics, University of Freiburg (Germany) funded by the German Federal Ministry of Education and Research BMBF grant 031 A538A de.NBI-RBC and the Ministry of Science, Research and the Arts Baden-Württemberg (MWK) within the framework of LIBIS/de.NBI Freiburg.

#### Appendix A. Supplementary data

Supplementary data to this article can be found online at https://doi. org/10.1016/j.bbagrm.2025.195104.

#### Data availability

ONT sequencing data was uploaded in the Sequence Read Archive as BioProject PRJNA1207539. Telomere-to-telomere zebrafish genomic assembly can be accessed at BioProject PRJNA1029986. The code for the analysis of transposon positions is available on Github (https://github.com/danio-elte/zfish transposon screen). version of the repository with the raw numerical data retrieved from the analysis of fluorescence intensity and an annotated GenBank file of the ctnnb2<sup>ich</sup> genomic sequence was uploaded to Zenodo as well [92].

#### References

- [1] S. Brantley, S.D. Talia, The maternal-to-zygotic transition, Curr. Biol. 34 (2024) R519-R523.
- N.L. Vastenhouw, W.X. Cao, H.D. Lipshitz, The maternal-to-zygotic transition revisited, Development 146 (2019) dev161471.
- E.W. Abrams, M.C. Mullins, Early zebrafish development: it's in the maternal genes, Curr. Opin. Genet. Dev. 19 (2009) 396–403.
- [4] R. Fuentes, B. Tajer, M. Kobayashi, J.L. Pelliccia, Y. Langdon, E.W. Abrams, M. C. Mullins. The maternal coordinate system: molecular-genetics of embryonic axis formation and patterning in the zebrafish, Curr. Top. Dev. Biol. 140 (2020) 341-389
- D.S. Johnston, C. Nüsslein-Volhard, The origin of pattern and polarity in the Drosophila embryo, Cell 68 (1992) 201-219
- E. Wieschaus, C. Nüsslein-Volhard, The Heidelberg screen for pattern mutants of Drosophila: a personal account, Annu Rev Cell Dev Bi 32 (2015) 1-46.

- [7] R. Dosch, D.S. Wagner, K.A. Mintzer, G. Runke, A.P. Wiemelt, M.C. Mullins, Maternal control of vertebrate development before the midblastula transition: mutants from the zebrafish I, Dev. Cell 6 (2004) 771-780.
- [8] C.E. Moravec, G.C. Voit, J. Otterlee, F. Pelegri, Identification of maternal-effect genes in zebrafish using maternal crispants, Development 148 (2021).
- [9] F. Pelegri, S. Schulte-Merker, A gynogenesis-based screen for maternal-effect genes in the zebrafish, *Danio rerio*, Methods Cell Biol. 60 (1999) 1–20.
- [10] F. Pelegri, M.P.S. Dekens, S. Schulte-Merker, H. Maischein, C. Weiler, C. Nüsslein-Volhard, Identification of recessive maternal-effect mutations in the zebrafish using a gynogenesis-based method, Dev. Dyn. 231 (2004) 324-335.
- [11] C. Kelly, A.J. Chin, J.L. Leatherman, D.J. Kozlowski, E.S. Weinberg, Maternally controlled (beta)-catenin-mediated signaling is required for organizer formation in the zebrafish, Development 127 (2000) 3899-3911.
- [12] H. Nojima, T. Shimizu, C.-H. Kim, T. Yabe, Y.-K. Bae, O. Muraoka, T. Hirata, A. Chitnis, T. Hirano, M. Hibi, Genetic evidence for involvement of maternally derived Wnt canonical signaling in dorsal determination in zebrafish, Mech. Dev. 121 (2004) 371-386.
- [13] H. Nojima, S. Rothhämel, T. Shimizu, C.-H. Kim, S. Yonemura, F.L. Marlow, M. Hibi, Syntabulin, a motor protein linker, controls dorsal determination, Development 137 (2010) 923-933.
- [14] Y.G. Langdon, M.C. Mullins, Maternal and zygotic control of zebrafish dorsoventral axial patterning, Annu. Rev. Genet. 45 (2011) 357-377.
- [15] X. Ge, D. Grotjahn, E. Welch, J. Lyman-Gingerich, C. Holguin, E. Dimitrova, E. W. Abrams, T. Gupta, F.L. Marlow, T. Yabe, et al., Hecate/Grip2a acts to reorganize the cytoskeleton in the symmetry-breaking event of embryonic axis induction, PLoS Genet. 10 (2014) e1004422.
- [16] M. Hibi, M. Takeuchi, H. Hashimoto, T. Shimizu, Axis formation and its evolution in ray-finned fish, in: K. Kobayashi, T. Kitano, Y. Iwao, M. Kondo (Eds.), Reproductive and Developmental Strategies. Diversity and Commonality in Animals, Springer, Tokyo, 2018, https://doi.org/10.1007/978-4-431-56609-0\_32.
- [17] F.-I. Lu, C. Thisse, B. Thisse, Identification and mechanism of regulation of the zebrafish dorsal determinant, Proc. Natl. Acad. Sci. USA 108 (2011) 15876-15880.
- [18] L.D. Tran, H. Hino, H. Quach, S. Lim, A. Shindo, Y. Mimori-Kiyosue, M. Mione, N. Ueno, C. Winkler, M. Hibi, et al., Dynamic microtubules at the vegetal cortex redict the embryonic axis in zebrafish, Development 139 (2012) 3644-3652.
- [19] G. Bellipanni, M. Varga, S. Maegawa, Y. Imai, C. Kelly, A.P. Myers, F. Chu, W. S. Talbot, E.S. Weinberg, Essential and opposing roles of zebrafish beta-catenins in the formation of dorsal axial structures and neurectoderm. Development 133 (2006) 1299–1309.
- [20] C. Cruz, S. Maegawa, E.S. Weinberg, S.W. Wilson, I.B. Dawid, T. Kudoh, Induction and patterning of trunk and tail neural ectoderm by the homeobox gene evel in zebrafish embryos, Proc. Natl. Acad. Sci. USA 107 (2010) 3564–3569.
- [21] S. Maegawa, M. Varga, E.S. Weinberg, FGF signaling is required for {beta}-cateninmediated induction of the zebrafish organizer, Development 133 (2006) 3265-3276.
- [22] S. Tanaka, H. Hosokawa, E.S. Weinberg, S. Maegawa, Chordin and dickkopf-1b are essential for the formation of head structures through activation of the FGF signaling pathway in zebrafish, Dev. Biol. 424 (2017) 189-197.
- [23] M. Tsang, S. Maegawa, A. Kiang, R. Habas, E. Weinberg, I.B. Dawid, A role for MKP3 in axial patterning of the zebrafish embryo, Development 131 (2004) 2769-2779.
- [24] M. Varga, S. Maegawa, G. Bellipanni, E.S. Weinberg, Chordin expression, mediated by nodal and FGF signaling, is restricted by redundant function of two betacatenins in the zebrafish embryo, Mech. Dev. 124 (2007) 775-791.
- [25] M. Varga, S. Maegawa, E.S. Weinberg, Correct anteroposterior patterning of the zebrafish neurectoderm in the absence of the early dorsal organizer, BMC Devi Biol. 11 (2011) 26.
- [26] S.-Y. Wu, J. Shin, D.S. Sepich, L. Solnica-Krezel, Chemokine GPCR signaling inhibits  $\beta$ -catenin during zebrafish axis formation, PLoS Biol. 10 (2012) e1001403.
- B. McClintock, The origin and behavior of mutable loci in maize, Proc. Natl. Acad. Sci. 36 (1950) 344-355.
- [28] A. Hayward, C. Gilbert, Transposable elements, Curr. Biol. 32 (2022) R904-R909. [29] M.K. Bhattacharyya, A.M. Smith, T.H.N. Ellis, C. Hedley, C. Martin, The wrinkled-
- seed character of pea described by Mendel is caused by a transposon-like insertion in a gene encoding starch-branching enzyme, Cell 60 (1990) 115-122.
- [30] A.E. van't Hof, P. Campagne, D.J. Rigden, C.J. Yung, J. Lingley, M.A. Quail, N. Hall, A.C. Darby, I.J. Saccheri, The industrial melanism mutation in British eppered moths is a transposable element, Nature 534 (2016) 102–105.
- [31] Z. Ivics, M.A. Li, L. Mátés, J.D. Boeke, A. Nagy, A. Bradley, Z. Izsvák, Transposonmediated genome manipulation in vertebrates, Nat. Methods 6 (2009) 415-422.
- [32] K. Kawakami, D.A. Largaespada, Z. Ivics, Transposons as tools for functional enomics in vertebrate models, Trends Genet. 33 (2017) 784-801.
- V. Korzh, Transposons as tools for enhancer trap screens in vertebrates, Genome Biol. 8 (2007) S8.
- [34] K.M. Kwan, E. Fujimoto, C. Grabher, B.D. Mangum, M.E. Hardy, D.S. Campbell, J. M. Parant, H.J. Yost, J.P. Kanki, C.-B. Chien, The Tol2kit: a multisite gateway based construction kit for Tol2 transposon transgenesis constructs, Dev. Dyn. 236 (2007) 3088-3099
- [35] G.K. Varshney, S.M. Burgess, Mutagenesis and phenotyping resources in zebrafish for studying development and human disease, Brief Funct Genom 13 (2014) 82-94.
- [36] D. Chalopin, M. Naville, F. Plard, D. Galiana, J.-N. Volff, Comparative analysis of transposable elements highlights mobilome diversity and evolution in vertebrates, Genome Biol. Evol. 7 (2015) 567-580.
- K. Howe, M.D. Clark, C.F. Torroja, J. Torrance, C. Berthelot, M. Muffato, J. E. Collins, S. Humphray, K. McLaren, L. Matthews, et al., The zebrafish reference

- genome sequence and its relationship to the human genome, Nature 496 (2013)
- [38] B. Gao, D. Shen, S. Xue, C. Chen, H. Cui, C. Song, The contribution of transposable elements to size variations between four teleost genomes, Mob. DNA 7 (2016) 4.
- [39] F. Shao, M. Han, Z. Peng, Evolution and diversity of transposable elements in fish genomes, Sci. Rep. 9 (2019) 15399.
- [40] F. Shao, M. Zeng, X. Xu, H. Zhang, Z. Peng, FishTEDB 2.0: an update fish transposable element (TE) database with new functions to facilitate TE research, Database 2024 (2024) baae044.
- [41] P. Bhat, L.E. Cabrera-Quio, V.A. Herzog, N. Fasching, A. Pauli, S.L. Ameres, SLAMseq resolves the kinetics of maternal and zygotic gene expression during early zebrafish embryogenesis, Cell Rep. 42 (2023) 112070.
- [42] L. Fishman, A. Modak, G. Nechooshtan, T. Razin, F. Erhard, A. Regev, J.A. Farrell, M. Rabani, Cell-type-specific mRNA transcription and degradation kinetics in zebrafish embryogenesis from metabolically labeled single-cell RNA-seq, Nat. Commun. 15 (2024) 3104.
- [43] G. da S. Pescador, D.B. Amaral, J.M. Varberg, Y. Zhang, Y. Hao, L. Florens, A. A. Bazzini, Protein profiling of zebrafish embryos unmasks regulatory layers during early embryogenesis, Cell Rep. 43 (2024) 114769.
- [44] D.S. Koos, R.K. Ho, The nieuwkoid gene characterizes and mediates a Nieuwkoop-center-like activity in the zebrafish, Curr. Biol. 8 (1998) 1199–1206.
- [45] S. Schneider, H. Steinbeisser, R.M. Warga, P. Hausen, Beta-catenin translocation into nuclei demarcates the dorsalizing centers in frog and fish embryos, Mech. Dev. 57 (1996) 191–198.
- [46] F. Valenti, J. Ibetti, Y. Komiya, M. Baxter, A.M. Lucchese, L. Derstine, C. Covaciu, V. Rizzo, R. Vento, G. Russo, et al., The increase in maternal expression of axin1 and axin2 contribute to the zebrafish mutant ichabod ventralized phenotype, J. Cell. Biochem. 116 (2015) 418–430.
- [47] A.J. Giraldez, Y. Mishima, J. Rihel, R.J. Grocock, S.V. Dongen, K. Inoue, A. J. Enright, A.F. Schier, Zebrafish MiR-430 promotes deadenylation and clearance of maternal mRNAs, Science 312 (2006) 75–79.
- [48] J.J.D. Ho, J.H.S. Man, J.H. Schatz, P.A. Marsden, Translational remodeling by RNA-binding proteins and noncoding RNAs, Wiley Interdiscip Rev: RNA 12 (2021) e1647.
- [49] C.E. Vejnar, M.A. Messih, C.M. Takacs, V. Yartseva, P. Oikonomou, R. Christiano, M. Stoeckius, S. Lau, M.T. Lee, J.-D. Beaudoin, et al., Genome wide analysis of 3' UTR sequence elements and proteins regulating mRNA stability during maternal-to-zygotic transition in zebrafish, Genome Res. 29 (2019) 1100–1114.
- [50] S. Houwing, L.M. Kamminga, E. Berezikov, D. Cronembold, A. Girard, H. van den Elst, D.V. Filippov, H. Blaser, E. Raz, C.B. Moens, et al., A role for Piwi and piRNAs in germ cell maintenance and transposon silencing in zebrafish, Cell 129 (2007) 69–82.
- [51] S. Houwing, E. Berezikov, R.F. Ketting, Zili is required for germ cell differentiation and meiosis in zebrafish, EMBO J. 27 (2008) 2702–2711.
- [52] L.J.T. Kaaij, S.W. Hoogstrate, E. Berezikov, R.F. Ketting, piRNA dynamics in divergent zebrafish strains reveal long-lasting maternal influence on zygotic piRNA profiles. RNA 19 (2013) 345–356.
- [53] C. Wei, L. Salichos, C.M. Wittgrove, A. Rokas, J.G. Patton, Transcriptome-wide analysis of small RNA expression in early zebrafish development, RNA 18 (2012) 915–929.
- [54] N.-C. Chang, Q. Rovira, J. Wells, C. Feschotte, J.M. Vaquerizas, Zebrafish transposable elements show extensive diversification in age, genomic distribution, and developmental expression, Genome Res. 32 (2022) 1408–1423.
- [55] M. Balik-Meisner, L. Truong, E.H. Scholl, R.L. Tanguay, D.M. Reif, Population genetic diversity in zebrafish lines, Mamm. Genome 29 (2018) 90–100.
- [56] Y. Deng, Y. Qian, M. Meng, H. Jiang, Y. Dong, C. Fang, S. He, L. Yang, Extensive sequence divergence between the reference genomes of two zebrafish strains, Tuebingen and AB, Mol. Ecol. Resour. 22 (2022) 2148–2157.
- [57] A. Amsterdam, R.M. Nissen, Z. Sun, E.C. Swindell, S. Farrington, N. Hopkins, Identification of 315 genes essential for early zebrafish development, Proc. Natl. Acad. Sci. USA 101 (2004) 12792–12797.
- [58] T. Kotani, K. Kawakami, Misty somites, a maternal effect gene identified by transposon-mediated insertional mutagenesis in zebrafish that is essential for the somite boundary maintenance, Dev. Biol. 316 (2008) 383–396.
- [59] S. Nagayoshi, E. Hayashi, G. Abe, N. Osato, K. Asakawa, A. Urasaki, K. Horikawa, K. Ikeo, H. Takeda, K. Kawakami, Insertional mutagenesis by the Tol2 transposon-mediated enhancer trap approach generated mutations in two developmental genes: tcf7 and synembryn-like, Development 135 (2007) 159–169.
- [60] G. Streisinger, F. Singer, C. Walker, D. Knauber, N. Dower, Segregation analyses and gene-centromere distances in zebrafish, Genetics 112 (1986) 311–319.
- [61] C. Feschotte, E.J. Pritham, DNA transposons and the evolution of eukaryotic genomes, Annu. Rev. Genet. 41 (2007) 331–368.
- [62] P. Sierra, R. Durbin, Identification of transposable element families from pangenome polymorphisms, Mob. DNA 15 (2024) 13.
- [63] C.A. Wilson, J.H. Postlethwait, A maternal-to-zygotic-transition gene block on the zebrafish sex chromosome, G3 (Bethesda) 14 (2024) jkae050.

- [64] C.A. Wilson, S.K. High, B.M. McCluskey, A. Amores, Y.-L. Yan, T.A. Titus, J. L. Anderson, P. Batzel, M.J. Carvan, M. Schartl, et al., Wild sex in zebrafish: loss of the natural sex determinant in domesticated strains, Genetics 198 (2014) 1201–1308
- [65] M.O. Schemberger, V.D. Nascimento, R. Coan, É. Ramos, V. Nogaroto, K. Ziemniczak, G.T. Valente, O. Moreira-Filho, C. Martins, M.R. Vicari, DNA transposon invasion and microsatellite accumulation guide W chromosome differentiation in a Neotropical fish genome, Chromosoma 128 (2019) 547–560.
- [66] Y. Liu, Z. Zhu, I.H.T. Ho, Y. Shi, J. Li, X. Wang, M.T.V. Chan, C.H.K. Cheng, Genetic deletion of miR-430 disrupts maternal-zygotic transition and embryonic body plan, Front. Genet. 11 (2020) 853.
- [67] A.A. Bazzini, F. del Viso, M.A. Moreno-Mateos, T.G. Johnstone, C.E. Vejnar, Y. Qin, J. Yao, M.K. Khokha, A.J. Giraldez, Codon identity regulates mRNA stability and translation efficiency during the maternal-to-zygotic transition, EMBO J. 35 (2016) 2087–2103
- [68] S.G. Medina-Muñoz, G. Kushawah, L.A. Castellano, M. Diez, M.L. DeVore, M.J. B. Salazar, A.A. Bazzini, Crosstalk between codon optimality and cis-regulatory elements dictates mRNA stability, Genome Biol. 22 (2021) 14.
- [69] Y. Mishima, Y. Tomari, Codon usage and 3' UTR length determine maternal mRNA stability in zebrafish, Mol. Cell 61 (2016) 874–885.
- [70] A.O. Subtelny, S.W. Eichhorn, G.R. Chen, H. Sive, D.P. Bartel, Poly(A)-tail profiling reveals an embryonic switch in translational control, Nature 508 (2014) 66–71.
- [71] B. Czech, M. Munafò, F. Ciabrelli, E.L. Eastwood, M.H. Fabry, E. Kneuss, G. J. Hannon, piRNA-guided genome defense: from biogenesis to silencing, Annu. Rev. Genet. 52 (2018) 131–157.
- [72] Y.W. Iwasaki, K. Shoji, S. Nakagwa, T. Miyoshi, Y. Tomari, Transposon-host arms race: a saga of genome evolution, Trends Genet. 41 (2025) 369–389.
- [73] D.M. Ozata, I. Gainetdinov, A. Zoch, D. O'Carroll, P.D. Zamore, PIWI-interacting RNAs: small RNAs with big functions, Nat. Rev. Genet. 20 (2019) 89–108.
- [74] L.P. Benoit Bouvrette, S. Bovaird, M. Blanchette, E. Lécuyer, oRNAment: a database of putative RNA binding protein target sites in the transcriptomes of model species, Nucleic Acids Res. 48 (2019) D166–D173.
- [75] P. Aleström, L. D'Angelo, P.J. Midtlyng, D.F. Schorderet, S. Schulte-Merker, F. Sohm, S. Warner, Zebrafish: housing and husbandry recommendations, Lab. Anim. 54 (2019) 213–224.
- [76] M. Westerfield, The Zebrafish Book A Guide for the Laboratory Use of Zebrafish (Danio rerio), 4th edition, University of Oregon Press, Eugene, 2000.
- [77] T.G. Community, L.A.L. Abueg, E. Áfgan, O. Allart, A.H. Awan, W.A. Bacon, D. Baker, M. Bassetti, B. Batut, M. Bernt, et al., The Galaxy platform for accessible, reproducible, and collaborative data analyses: 2024 update, Nucleic Acids Res. 52 (2024) W83–W94.
- [78] M. Kolmogorov, J. Yuan, Y. Lin, P.A. Pevzner, Assembly of long, error-prone reads using repeat graphs, Nat. Biotechnol. 37 (2019) 540–546.
- [79] M. Alonge, L. Lebeigle, M. Kirsche, K. Jenike, S. Ou, S. Aganezov, X. Wang, Z. B. Lippman, M.C. Schatz, S. Soyk, Automated assembly scaffolding using RagTag elevates a new tomato system for high-throughput genome editing, Genome Biol. 23 (2022) 258.
- [80] H. Li, New strategies to improve minimap2 alignment accuracy, Bioinformatics 37 (2021) 4572–4574.
- $[81] \ \ Benchling \ [Biology \ Software], \ Retrieved \ from, \ \ \ \ https://benchling.com, \ 2025.$
- [82] N.D. Meeker, S.A. Hutchinson, L. Ho, N.S. Trede, Method for isolation of PCR-ready genomic DNA from zebrafish tissues, BioTechniques 43 (2007), 610-612-614.
- [83] H. Ogawa, K. Umesono, Intracellular localization and transcriptional activation by the human glucocorticoid receptor-green fluorescent protein (GFP) fusion proteins, Acta Histochem. Cytochem. 31 (2010) 303.
- [84] J. Schindelin, I. Arganda-Carreras, E. Frise, V. Kaynig, M. Longair, T. Pietzsch, S. Preibisch, C. Rueden, S. Saalfeld, B. Schmid, et al., Fiji: an open-source platform for biological-image analysis, Nat. Methods 9 (2012) 676–682.
- [85] S.F. Altschul, W. Gish, W. Miller, E.W. Myers, D.J. Lipman, Basic local alignment search tool, J. Mol. Biol. 215 (1990) 403–410.
- [86] M. Lawrence, W. Huber, H. Pagès, P. Aboyoun, M. Carlson, R. Gentleman, M. T. Morgan, V.J. Carey, Software for computing and annotating genomic ranges, PLoS Comput. Biol. 9 (2013) e1003118.
- [87] Z. Gu, L. Gu, R. Eils, M. Schlesner, B. Brors, Circlize implements and enhances circular visualization in R, Bioinformatics 30 (2014) 2811–2812.
- [88] Q. Wang, M. Li, T. Wu, L. Zhan, L. Li, M. Chen, W. Xie, Z. Xie, E. Hu, S. Xu, et al., Exploring epigenomic datasets by ChIPseeker, Curr Protoc 2 (2022) e585.
- [89] G. Yu, L.-G. Wang, Q.-Y. He, ChiPseeker: an R/Bioconductor package for ChiP peak annotation, comparison and visualization, Bioinformatics 31 (2015) 2382–2383.
- [90] R Core Team, R: A Language and Environment for Statistical Computing, R Foundation for Statistical Computing, Vienna, Austria, 2021. https://www.R-pro.iect.org/
- [91] H. Wickham, ggplot2: Elegant Graphics for Data Analysis, Springer-Verlag, New York, 2016. ISBN 978-3-319-24277-4, https://ggplot2.tidyverse.org.
- [92] Z. Varga, F. Kagan, S. Maegawa, Á. Nagy, J. Okendo, S.M. Burgess, E.S. Weinberg, M. Varga, Data Related to the Mapping of the Maternal Effect Zebrafish *ichabod* Mutation Creators, Zenodo, 2025.